Contrast enhanced high-resolution diffuse optical tomography of the human brain using ICG

Christina Habermehl[1,*], Christoph H. Schmitz[1,2], and Jens Steinbrink[1,3]

[1]*Berlin NeuroImaging Center, Charité University Hospital, Department of Neurology, Charitéplatz 1, 10117 Berlin, Germany*

[2] *NIRx Medizintechnik GmbH, Baumbachstr. 17, 13189 Berlin, Germany*

[3] *Center for Strokeresearch Berlin (CSB), Charité University Hospital, 10098 Berlin, Germany*

** christina.habermehl@charite.de*

Abstract: Non-invasive diffuse optical tomography (DOT) of the adult brain has recently been shown to improve the spatial resolution for functional brain imaging applications. Here we show that high-resolution (HR) DOT is also advantageous for clinical perfusion imaging using an optical contrast agent. We present the first HR-DOT results with a continuous wave near infrared spectroscopy setup using a dense grid of optical fibers and indocyanine green (ICG) as an exogenic contrast agent. We find an early arrival of the ICG bolus in the intracerebral tissue and a delayed arrival of the bolus in the extracerebral tissue, achieving the separation of both layers. This demonstrates the method's potential for brain perfusion monitoring in neurointensive care patients.

OCIS codes: (170.2655) Functional monitoring and imaging; (170.6280) Spectroscopy, fluorescence and luminescence; (170.6960) Tomography.

References and links

1. P. Hopton, T. S. Walsh, and A. Lee, "Measurement of cerebral blood volume using near-infrared spectroscopy and indocyanine green elimination," J. Appl. Physiol. **87**(5), 1981–1987 (1999).
2. E. Keller, A. Nadler, H. Alkadhi, S. S. Kollias, Y. Yonekawa, and P. Niederer, "Noninvasive measurement of regional cerebral blood flow and regional cerebral blood volume by near-infrared spectroscopy and indocyanine green dye dilution," Neuroimage **20**(2), 828–839 (2003).
3. C. Terborg, S. Bramer, S. Harscher, M. Simon, and O. W. Witte, "Bedside assessment of cerebral perfusion reductions in patients with acute ischaemic stroke by near-infrared spectroscopy and indocyanine green," J. Neurol. Neurosurg. Psychiatry **75**(1), 38–42 (2004).
4. C. Terborg, K. Gröschel, A. Petrovitch, T. Ringer, S. Schnaudigel, O. W. Witte, and A. Kastrup, "Noninvasive assessment of cerebral perfusion and oxygenation in acute ischemic stroke by near-infrared spectroscopy," Eur. Neurol. **62**(6), 338–343 (2009).
5. A. Liebert, H. Wabnitz, H. Obrig, R. Erdmann, M. Möller, R. Macdonald, H. Rinneberg, A. Villringer, and J. Steinbrink, "Non-invasive detection of fluorescence from exogenous chromophores in the adult human brain," Neuroimage **31**(2), 600–608 (2006).
6. A. Liebert, H. Wabnitz, J. Steinbrink, H. Obrig, M. Möller, R. Macdonald, A. Villringer, and H. Rinneberg, "Time-resolved multidistance near-infrared spectroscopy of the adult head: intracerebral and extracerebral absorption changes from moments of distribution of times of flight of photons," Appl. Opt. **43**(15), 3037–3047 (2004).
7. M. Kohl-Bareis, H. Obrig, J. Steinbrink, J. Malak, K. Uludag, and A. Villringer, "Noninvasive monitoring of cerebral blood flow by a dye bolus method: separation of brain from skin and skull signals," J. Biomed. Opt. **7**(3), 464–470 (2002).
8. R. L. Barbour, H. L. Graber, Y. Pei, S. Zhong, and C. H. Schmitz, "Optical tomographic imaging of dynamic features of dense-scattering media," J. Opt. Soc. Am. A **18**(12), 3018–3036 (2001).
9. A. Bluestone, G. Abdoulaev, C. Schmitz, R. Barbour, and A. Hielscher, "Three-dimensional optical tomography of hemodynamics in the human head," Opt. Express **9**(6), 272–286 (2001).

#153631 - $15.00 USD Received 31 Aug 2011; accepted 31 Aug 2011; published 8 Sep 2011

10. D. A. Boas, K. Chen, D. Grebert, and M. A. Franceschini, "Improving the diffuse optical imaging spatial resolution of the cerebral hemodynamic response to brain activation in humans," Opt. Lett. **29**(13), 1506–1508 (2004).
11. B. R. White and J. P. Culver, "Quantitative evaluation of high-density diffuse optical tomography: in vivo resolution and mapping performance," J. Biomed. Opt. **15**(2), 026006 (2010).
12. S. P. Koch, C. Habermehl, J. Mehnert, C. H. Schmitz, S. Holtze, A. Villringer, J. Steinbrink, and H. Obrig, "High-resolution optical functional mapping of the human somatosensory cortex," Front Neuroenergetics **2**, 12 (2010).
13. T. Desmettre, J. M. Devoisselle, S. Soulie-Begu, and S. Mordon, "[Fluorescence properties and metabolic features of indocyanine green (ICG)]," J. Fr. Ophtalmol. **22**(9), 1003–1016 (1999).
14. M. L. Landsman, G. Kwant, G. A. Mook, and W. G. Zijlstra, "Light-absorbing properties, stability, and spectral stabilization of indocyanine green," J. Appl. Physiol. **40**(4), 575–583 (1976).
15. E. Keller, H. Ishihara, A. Nadler, P. Niederer, B. Seifert, Y. Yonekawa, and K. Frei, "Evaluation of brain toxicity following near infrared light exposure after indocyanine green dye injection," J. Neurosci. Methods **117**(1), 23–31 (2002).
16. Y. Pei, H. L. Graber, and R. L. Barbour, "Influence of Systematic Errors in Reference States on Image Quality and on Stability of Derived Information for dc Optical Imaging," Appl. Opt. **40**(31), 5755–5769 (2001).
17. C. H. Schmitz, H. L. Graber, H. Luo, I. Arif, J. Hira, Y. Pei, A. Bluestone, S. Zhong, R. Andronica, I. Soller, N. Ramirez, S. L. Barbour, and R. L. Barbour, "Instrumentation and calibration protocol for imaging dynamic features in dense-scattering media by optical tomography," Appl. Opt. **39**(34), 6466–6486 (2000).
18. H. Obrig, M. Neufang, R. Wenzel, M. Kohl, J. Steinbrink, K. Einhäupl, and A. Villringer, "Spontaneous low frequency oscillations of cerebral hemodynamics and metabolism in human adults," Neuroimage **12**(6), 623–639 (2000).

1. Introduction

In neurointensive care, bedside monitoring of brain perfusion or perfusion based therapies is desirable to evaluate the patient's pathologic state and to guide treatment. Existing imaging modalities such as X-ray computed tomography, magnet resonance imaging (MRI) or positron emission tomography are not always within a timely reach to the intensive care unit (ICU) and are not suited for constant monitoring of the brain. Furthermore, imaging facilities may be remote from the ICU and require undesirable intensive-care patient transport. Other established neurological monitoring techniques like intracranial pressure assessment, microdialysis and transcranial Doppler ultrasonography cannot monitor perfusion of the brain parenchyma.

Contrast enhanced near infrared spectroscopy (NIRS) has the potential to close this gap and serve as a quasi-continuous brain perfusion monitor. It is portable, noninvasive, and may be applied regularly (e.g. every 20-60 min) without undue discomfort or adverse health effects. Previous NIRS studies of brain perfusion using indocyanine green (ICG) focused on the measurement of cerebral blood flow (CBF) and cerebral blood volume (CBV) [1,2] or differences of bolus kinetics in affected and unaffected hemispheres in stroke patients [3,4]. All these studies employed a topographic NIRS approach, which uses next-nearest neighbor measurements of optical fibers that are equally separated up to 5 cm. One major challenge of this approach is that the signal of the contrast agent in superficial layers like skin can dominate the measured absorption change. That's why methods are needed that are able to differentiate between tissue depths and that assess the contribution of the signal that originates from the brain.

Studies using depth resolved NIRS, like time-domain (TD) [5,6] and frequency-domain (FD) techniques [7] have shown the passage of an ICG bolus in the brain. Consistently, it was found that in healthy subjects the bolus was detected first in deeper (cerebral) layers and a few seconds later in the superficial (skin) layers. Signals from intracerebral tissue declined faster than signals from superficial layers. This is in good agreement with the known high perfusion of brain tissue, and this phenomenon allows evaluating the separation of intra- and extracerebral fractions of the signal. While these FD and TD results are promising, we believe that the introduction into clinical use would benefit greatly from the application of continuous wave (cw) DOT, which is technically much less demanding and more economic compared to other approaches. In this study, we used a cw DOT system with a dense optical fiber set-up to

#153631 - $15.00 USD Received 31 Aug 2011; accepted 31 Aug 2011; published 8 Sep 2011

detect absorption changes caused by an injected ICG bolus. DOT is based on acquiring NIRS signals from different inter-optode distances, which facilitates the measurement of overlapping photon paths [8,9] and thereby provides an enhanced lateral and an additional depth resolution [10,11]. In our specific case, we use a dense grid of optical fibers with less than 10 mm optode separation, affording HR-DOT images [12].

We are the first to demonstrate the bolus kinetics of an ICG injection using a cw HR-DOT system. We visualize the different bolus kinetics in the several compartments of the head, demonstrating the separation of intra-and extracerebral tissue, thus confirming the results that were obtained with more complex imaging devices. This is a contribution to the attempt of many research groups to develop a bedside-monitoring tool for brain perfusion. In contrast to other groups we do not aim for measuring absolute values of CBF or CBV which may not be necessary when the patient is repeatedly monitored.

2. Methods

ICG is a non-toxic fluorescent dye [13] that binds tightly to serum proteins and has been frequently used in clinical routine. ICG absorbs light in the near infrared spectrum with an absorption and emission maximum at 805 nm in plasma solution [14]. Stroke patients often suffer from a disruption of the blood-brain-barrier (BBB). In experimental stroke models, it was shown that a disturbance of the BBB together with an ICG injection and the exposure to near-infrared light does not lead to photo toxicity [15].

We investigated three healthy, voluntary subjects (2 male, mean age 38 years), all authors of this work. We administered 25 mg indocyanine green (ICG-PULSION, PULSION Medical Systems, Germany), diluted in 15 ml of saline into the cubital vein of the right arm. Subject 1 received two boli (9 mg ICG as the first bolus, 16 mg as the second bolus) with a 10 min delay. Subject 2 and 3 were administered one bolus of 12.5 mg ICG each.

Absorption changes were measured using the DYNOT tomography imager (NIRx Medizintechnik GmbH, Berlin, Germany), applying light of two wavelengths (λ = 760 nm & λ = 830 nm) to the subject's head. 30 co-located optical fibers (inter-optode separation: 7.5 mm), each serving as source and detector, were placed in a 5 x 6 optical fiber grid covering ~12 cm^2 of the right hemisphere (see, Fig. 1a, b). With this dense fiber grid setup we obtained 900 overlapping optical data channels. To fixate the optical fibers on the head surface and to ensure stable optical contact, the system uses an open scaffolding structure and individually spring-loaded fibers. This design allows easy access of the fiber tips for parting of the hair before placing an optode.

A time series of relative absorption changes within the investigated volume was reconstructed using a commercial software (NAVI, NIRx Medical Technology LLC, Glen Head, NY, USA). This software applies the normalized difference method described in [16]. This algorithm linearizes the reconstruction problem by applying a perturbation approach, thereby reducing the imaging problem to an inversion of the weight function.

The weight matrix was determined using BrainModeler (NIRx Medical Technology LLC) which provides a library of subvolumes from a MRI-scan based finite element mesh with precalculated inverse parameters for all possible source and detector combinations on the subvolume's boundary (see, Fig. 1c, d). Each of these subvolumes contains precalculated forward solutions of the photon diffusion equation and reference detector values. These are computed based on the simplified assumption of homogenous interior optical properties (μ_a = 0.06 cm^{-1}, μ_s = 10 cm^{-1}).

#153631 - $15.00 USD Received 31 Aug 2011; accepted 31 Aug 2011; published 8 Sep 2011

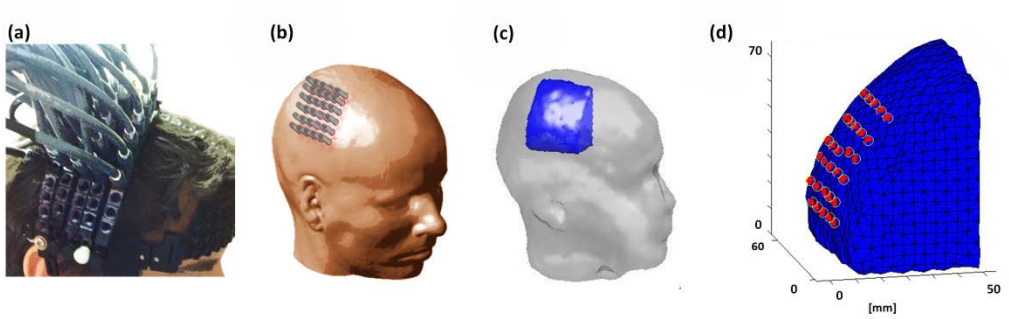

Fig. 1. Imaging setup. (a) Absorption changes were measured with a DOT imaging system (DYNOT, NIRx Medizintechnik GmbH, Berlin, Germany) (b) A 5x6 fiber grid with 30 co-located sources and detectors was placed pericentrally over the right hemisphere. (c), (d) Finite element mesh that was used for image reconstruction of relative absorption changes. Red dots indicate the positions of the optical fibers in the forward geometry.

All data were low-pass filtered to reduce cardiac and high-frequency noise before further processing (f_{cutoff} = 0.3 Hz). In a first step we evaluated the depth sensitivity of the different source-detector (SD) distances for which we averaged the detector readings from all 1st nearest neighbor (NN) and all 3rd NN measurements. These time courses were corrected to a baseline 10 sec prior to the bolus injection (at t = 0 s) and normalized to their minimum values after bolus answer (t = 5-30 s).

Secondly we reconstructed time courses of absorption changes from different depths of the reconstruction volume. These time courses were also baseline corrected and normalized to their maximum values after bolus injection (t = 5-30 s). This allows for a direct comparison of the bolus kinetics within the different tissue depths.

#153631 - $15.00 USD Received 31 Aug 2011; accepted 31 Aug 2011; published 8 Sep 2011

3. Results

3.1 An earlier increase in absorption can be observed for larger optode distances

Three-dimensional DOT uses multi-distance measurements of different SD combinations. Light that is detected far away from the source is assumed to have passed deeper tissue layers than light that is detected close to the source. Signals measured with 3rd NN combinations (~22.5 mm SD distance) can be assumed to have significant components originating from brain tissue, while signals from 1st NN (~7.5 mm SD distance) channels contain mainly information of skin and skull tissue.

When examining the raw detector readings (not shown), we find an averaged decrease in the measured intensity of 8% for 1st NN and 12% for 3rd NN combinations (standard deviation of a 45 s pre-bolus baseline: 0.5% for 1st NN and 0.8% for 3rd NN).

To compare the different bolus kinetics directly, Fig. 2 shows normalized detector readings from 1st NN and 3rd NN measurements (data from subject 1, 1st bolus and $\lambda = 760$ nm). The averaged 1st NN response (red) shows a clear delay in the bolus-related signal decrease, compared to the mean 3rd NN signal (blue). This is explained because the larger optode separations have a significant signal contribution from deep tissue (i.e., cortex), which due to better perfusion is reached first by the bolus compared to skin. Short SD separations, in contrast, are much less sensitive to deep tissue and are mainly influenced by superficial activity, such as skin perfusion, which is known to be delayed with respect to the brain. This clearly demonstrates the sensitivity of the different SD distances to different tissue depths, even in the raw (non-reconstructed) signals.

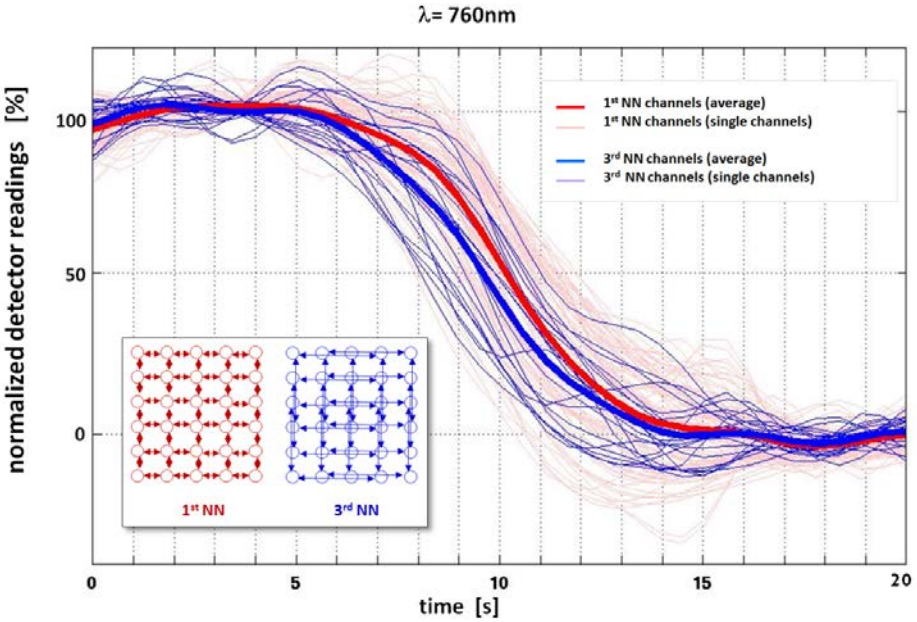

Fig. 2. Normalized detector readings following an ICG bolus (subject 1, $\lambda = 760$ nm). Red lines indicate the time course of all 1st NN combinations (SD distance 7.5 mm). Blue lines represent the time course for all 3rd NN combinations (SD distance 22.5 mm). The average of all 1st NN and 3rd NN time courses is given in bold. Box in the left corner depicts the fiber grid set-up and the channels taken for the different time courses.

#153631 - $15.00 USD Received 31 Aug 2011; accepted 31 Aug 2011; published 8 Sep 2011

3.2 Reconstruction in DOT allows the separation of extra- and intra-cerebral tissue

To be able to locate the bolus dynamics in a volumetric view, we reconstructed a three-dimensional time series of absorption changes within the sampled tissue, using the forward geometry and definition of the optical fiber arrangement shown in Fig. 1d.

Figure 3a and supplementary Media 1 depict a frontal view on the reconstructed result volume, visualizing the early arrival of ICG in deeper voxels at t = 5 s and the arrival of the dye in superficial layers approximately at t = 7 s. Figure 3b shows the arrival time of the bolus in each voxel by color-coding the time at which 50% of the maximum absorption value is reached. In both figures we find a clear border at a depth of 10-12 mm, beneath which the early response is seen. This indicates the location of the cortical surface that runs about 10-14 mm blow the head surface (see, Fig. 3c).

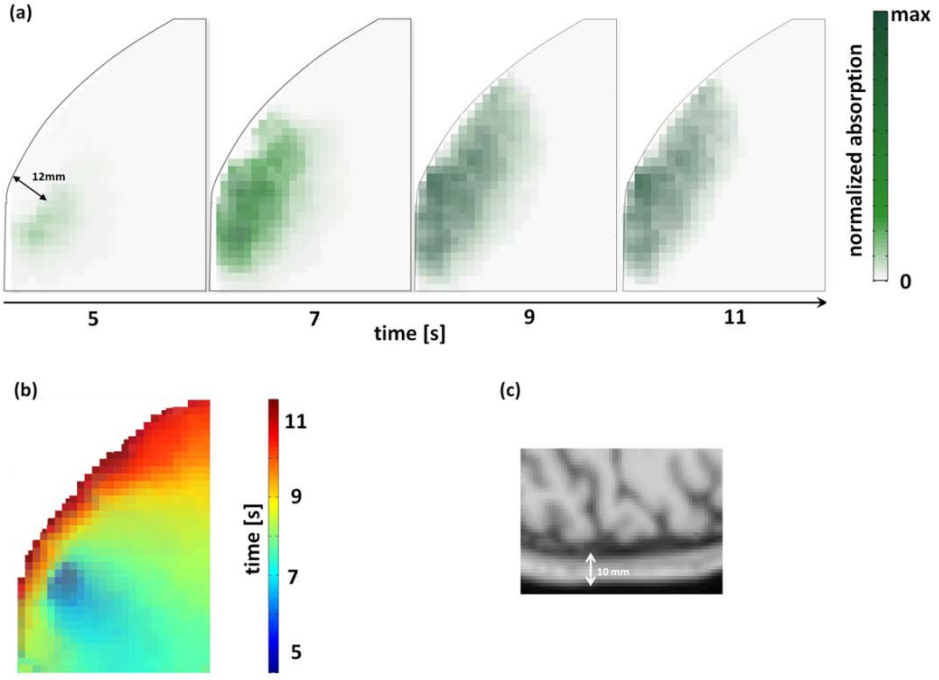

Fig. 3. (a) Single frames from a video (Media 1), depicting the frontal view on the reconstructed result volume (subject 1, 1st ICG bolus and λ = 760 nm). Green voxels indicate increased absorption. Voxels are colored semi-transparent, bolus injection was at t = 0-1 s. (b) Same view on the reconstructed result volume as in (a), displaying for each voxel the time (in s after bolus injection) when 50% of the maximum absorption value was reached. (c) Transversal slice from an anatomical scan of the used forward model geometry.

Figure 4 shows the averaged reconstructed time courses from two regions of interest (ROI) of different tissue depth for subject 1. One ROI is located in the superficial (skin) layer (red), and the other one in the brain region (blue). Since the image reconstruction procedure calculates relative changes of absorption, the baseline - prior to the bolus - fluctuates around zero. The measured relative increase of absorption due to the bolus injection ranged between $1.0*10^{-5}$ and $2.6*10^{-5}$ mol/l for deep voxels and $1.3*10^{-5}$ and $2.4*10^{-5}$ mol/l for superficial voxels. To allow for a direct comparison of the different bolus kinetics, we normalized each time course to its maximum value directly after bolus answer (t = 5-30 s).

In both boli of subject 1 and for each wavelength we find a systematic earlier increase of absorption in deeper voxels and delayed (1.5-4 s) increase of absorption within the superficial layer. We also observe a fast decline in the time courses of the deeper voxels. This

#153631 - $15.00 USD Received 31 Aug 2011; accepted 31 Aug 2011; published 8 Sep 2011

observation is in line with contrast enhanced perfusion-weighted MRI and has also been observed using FD and TD systems [6,7].

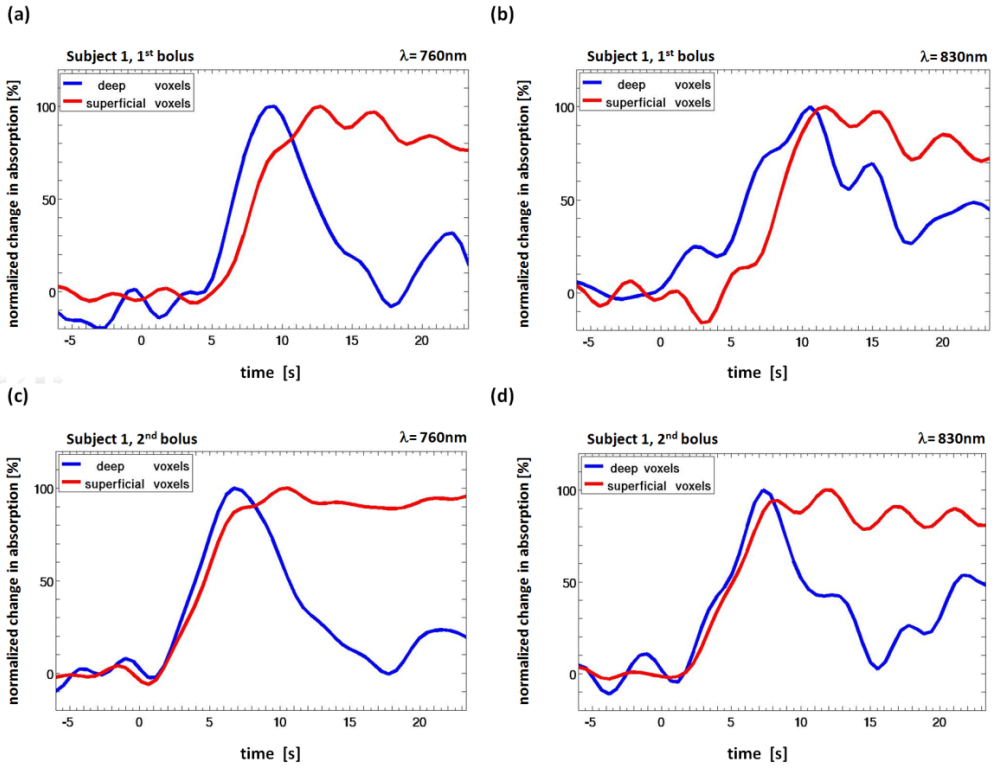

Fig. 4. Time courses of normalized relative absorption changes for subject 1 and both boli and wavelengths. Red lines represent the averaged intensity values from superficial voxels; blue lines represent intensity values from voxels from deeper (cortical) layers. Injection of the ICG bolus was at t = 0-1s. Note, that due to manual injection, this time point is only an approximation. (a) 1st ICG bolus, λ = 760 nm. (b) 1st bolus, λ = 830 nm. (c) 2nd bolus, λ = 760 nm. (d) 2nd bolus, λ = 830 nm.

Figure 5 presents the results for subject 2 and subject 3, demonstrating the robustness of the method. Similar to the results of subject 1 we can clearly separate deeper voxels with an early arrival of the absorber and superficial voxels with a later increase of absorption. Due to the somewhat slower injection of the bolus we find a more broadened answer in the deeper voxels than in subject 1.

We determined the characteristic shape in the time courses of the in- and out-flow of the contrast agent in extra-and intracerebral tissue in all three subjects, demonstrating that three-dimensional perfusion imaging of the brain is possible using cw HR-DOT.

#153631 - $15.00 USD Received 31 Aug 2011; accepted 31 Aug 2011; published 8 Sep 2011

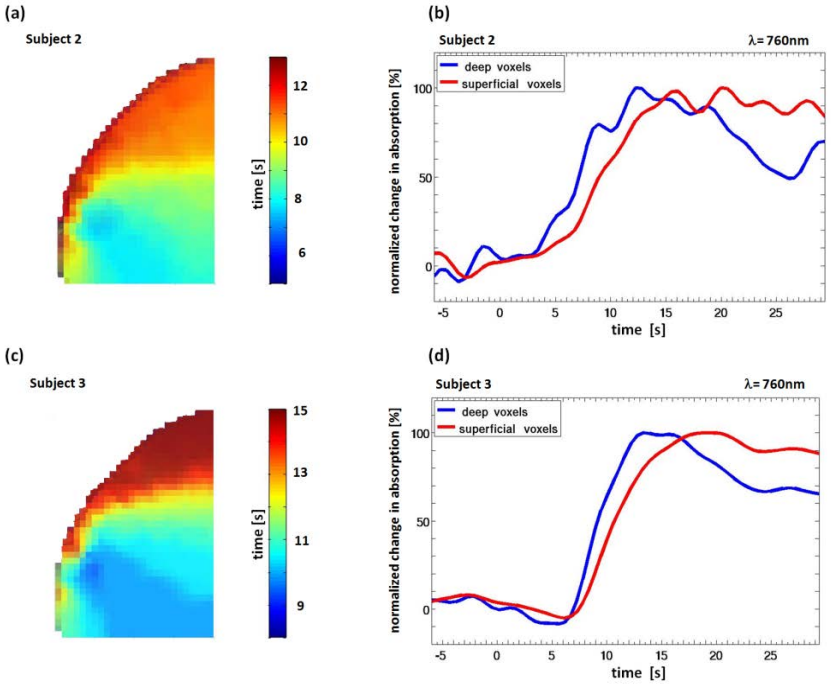

Fig. 5. (a) Subject 2. Frontal view on the reconstruction volume, color-coded voxels depict the time (in s after bolus injection (t = 0-3 s)) when 50% of the maximum absorption value was reached. (b) Subject 2, reconstructed time courses for deep and superficial voxels for λ = 760 nm. (c), (d) Same as (a), (b) but for subject 3.

To show the improved resolution of the method, Fig. 6 and Media 2 present a secondary result. When viewing the HR-DOT images for subject 1 in an angle perpendicular to the head surface, we consistently observe a distinct pattern of the arriving absorber in the most superficial layer. The bolus dynamics in the outermost layer (10 mm thickness) displays the arrival of the ICG at t = 7 sec, spreading from anterior/inferior to posterior/superior. These results were confirmed for every bolus injection and wavelength (data only shown for 1st bolus and λ = 760 nm). This is further indication of the excellent lateral and depth resolution of the used imaging system and reconstruction procedure.

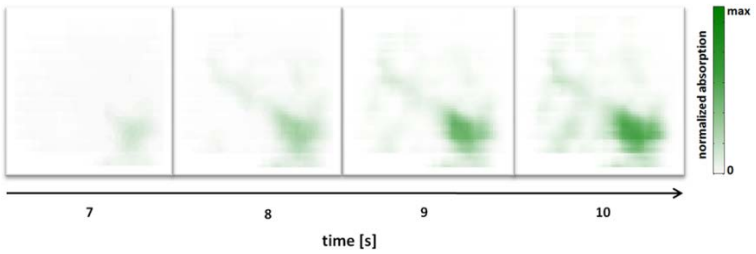

Fig. 6. Single frames from a video (Media 2) of a lateral view on a 10 mm thick slice (60 x 60 mm wide) of superficial layers for subject 1, the 1st ICG bolus and λ = 760 nm. Green voxels indicate increased absorption.

4. Discussion and conclusion

Monitoring of cerebral perfusion in neurointensive care is highly desirable and as of yet is only partially realized owing to the scarcity of neuro-ICU equipped with dedicated imaging

#153631 - $15.00 USD Received 31 Aug 2011; accepted 31 Aug 2011; published 8 Sep 2011

equipment on one hand, and the limited monitoring capability of existing equipment on the other. A tool that enables the regular monitoring at short intervals at the bedside using a safe dye would be helpful, also because many patients cannot easily be transported. Unlike topographic NIRS, we demonstrate that the cw HR-DOT has sufficient depth and lateral resolution to be used for cerebral perfusion monitoring. It furthermore overcomes the technical challenges of more demanding FD or TD NIRS approaches.

In this study, we investigated the feasibility of separating intra- and extracerebral tissue by using a cw HR-DOT imaging system which is normally used to determine concentration changes of oxy- (HbO) and deoxygenated (HbR) hemoglobin [12,17] due to brain activation. We were able to reproduce previous results [6,7] with a less demanding system in all three subjects. Three-dimensional result volumes of absorption changes were reconstructed within a few seconds due to the use of pre-calculated forward solutions. The images show a high lateral and good depth resolution and allow the separation of intra- and extracerebral tissue.

The used wavelengths are close to the maximal absorption spectrum of ICG in plasma. We are aware of the fact that there are three chromophores that mainly contribute to the measured signal, but the impact of changes in HbO and HbR concentration (which can be seen in fluctuations of the baseline) is relatively small and stable over time compared to the high amplitude changes in light attenuation caused by the ICG. For example, referring the measurement with $\lambda = 760$ nm (subject 1, bolus 1, intracerebral ROI) we found an almost 10-fold increased amplitude of the ICG response ($1.1*10^{-5}$ mol/l) compared to the standard deviation of a 45s pre-bolus baseline ($1.2*10^{-6}$ mol/l). For $\lambda = 830$ nm (same measurement) we found a more than 20-fold increase.

Nevertheless, hemodynamics can be observed in the signal; especially within the 830 nm time courses, to which HbO is the predominantly contributing hemoglobin species, we see oscillations that are part of systemic signals [18]. For further studies, we consider the implementation of a third wavelength, allowing for a better separation of the signals. However, the typical bolus kinetics with different bolus arrival times within the different compartments and the fast decline of the signal within cerebral tissue and can clearly be seen using a single wavelength. The distinct border of the early arrived bolus at 12 mm tissue depth indicates the cerebral boundary.

In this study we succeeded in the attempt of showing the separation of intra- and extracerebral tissue by using a cw HR-DOT imaging system in combination with the injection of a safe dye. In our results, we see the early arrival of the ICG for larger SD-separations in the raw data and the expected bolus kinetics in different layers of the reconstructed volume. This work can help to promote the use of DOT for monitoring patients undergoing brain trauma or stroke. It could be highly usefull to detect changes in brain perfusion in time without expensive measurements and difficult transport of the patient. We highly recommend further studies using a more complex system that takes changes of all important chromophores into account.

Acknowledgements

This work was supported in part under NIH Grant Nos. R42NS050007 and R44NS049734 and by the National Bernstein Network Computational Neuroscience, Bernstein Focus: Neurotechnology, No. 01GQ0850, Project B3. We kindly thank Dr. Alexander Pöllinger for helping us to conduct the experiment.